

- plants grow at a higher temperature (9).
13. The terminal flowers of *ttf1* mutant plants often vary in their organ numbers and arrangement relative to wild-type flowers (8, 9, 11). Wild-type flowers are composed of four whorls of organs: four sepals outermost, four petals, six stamens, and two central, fused carpels. In *ttf1* mutants, the terminal flower and one or two flowers generated below may be partially united at the apex. Organ primordia may arise in a mix of whorls and spirals, with some organs apparently fused together. Mosaic organs may occur, with patches of one floral organ type mixed with another. The number of each organ type is often less than in the wild type, though carpels are usually normal.
  14. An *Arabidopsis* genomic clone was obtained by screening a Landsberg *erecta* library [G. C. Whitelam *et al.*, *Plant Cell* **5**, 757 (1993)] with the *CEN* cDNA (7). About 80,000 recombinants were screened at 60°C and washed at 60°C with 0.4× SSC and 0.5% SDS, as described (22). Of five positives, one yielded a 14-kb Xba I fragment that was subcloned into Bluescript KS+ vector (Stratagene) to give pJAM2043. A 2-kb Eco RI-Xba I fragment of pJAM2043 contained all of the *CEN*-hybridizing signal and was subcloned as pJAM2044.
  15. Database searches involved BLAST [S. F. Altschul, W. Gish, W. Miller, E. W. Myers, D. J. Lipman, *J. Mol. Biol.* **215**, 403 (1990)] and FASTA [W. R. Pearson and D. J. Lipman, *Proc. Natl. Acad. Sci. U.S.A.* **85**, 2444 (1988)]. The *Arabidopsis* clone 129D777 was obtained from the Arabidopsis Biological Resource Center at Ohio State University (Columbus, OH) and was originally isolated from *Arabidopsis thaliana* ecotype Columbia; see T. Newman *et al.* at Michigan State University (East Lansing, MI) (accession number T44654).
  16. The *Arabidopsis* EST was mapped to the top of chromosome 5, above the restriction fragment length polymorphism marker 447 (R. Schmidt, personal communication), in agreement with previous mapping (8, 9).
  17. Wild-type *Arabidopsis* (Columbia) and plants carrying alleles *ttf1-1*, *ttf1-11*, *ttf1-13*, or *ttf1-14* were grown on soil under LD. Seeds carrying *ttf1* alleles were obtained from the Arabidopsis Biological Resource Center at Ohio State University. Genomic DNA was isolated from wild-type and mutant plants by means of a miniprep method (R. Simon, personal communication). Leaf tissue was homogenized while frozen, buffer [50 mM EDTA, 0.1 M tris-HCl (pH 8), and 1% SDS] was added, and the sample was thawed at 65°C for 2 min. DNA was extracted with phenol, phenol/chloroform (1:1), and chloroform, and precipitated with isopropanol and sodium acetate. After an ethanol wash, DNA was resuspended in tris-EDTA containing ribonuclease. Oligonucleotide primers were designed to sequences ~160 bp upstream of the ATG and 120 bp downstream of the stop codon. To avoid polymerase chain reaction (PCR) artifacts, we carried out three separate PCRs on each DNA preparation and cloned one PCR product from each into pGEM-T vector (Promega). Each clone of ~1.3 kb was sequenced using the ABI Prism system (Perkin-Elmer), and only base changes present in all three PCR products for any one allele were considered genuine.
  18. The rice clone S19461A was obtained from the National Institute of Agrobiological Resource Rice Genome Resource Project (RGP), Ibaraki, Japan, and was isolated from *Oryza sativa* (GenBank accession number D40166). The partial sequence of the rice clone R29181A (GenBank accession number D24998) was made by M. Yuzo and S. Takuji (RGP, Ibaraki, Japan) and was obtained from the databases (15).
  19. D. K. Grandy *et al.*, *Mol. Endocrinol.* **4**, 1370 (1990); S. Bucquoy, P. Jolles, F. Schoentgen, *Eur. J. Biochem.* **225**, 1203 (1994).
  20. D. Weigel, J. Alvarez, D. R. Smyth, M. F. Yanofsky, E. M. Meyerowitz, *Cell* **69**, 843 (1992); D. Weigel and O. Nilsson, *Nature* **377**, 495 (1995).
  21. D. Bradley, O. Ratcliffe, C. Vincent, R. Carpenter, E. Coen, data not shown.
  22. D. Bradley, R. Carpenter, H. Sommer, N. Hartley, E. Coen, *Cell* **72**, 85 (1993).
  23. Sequence alignment programs used the GCG package (University of Wisconsin).
  24. Wild-type plants of *Arabidopsis thaliana* ecotype Columbia were grown under 16 hours light/8 hours dark and harvested just as plants showed signs of bolting. Methods for digoxigenin labeling of RNA probes, tissue preparation, and in situ hybridization were as described [see (22)]. Double labeling first involved digoxigenin-labeled antisense *TFL1* RNA and purple color detection, followed by fluorescein isothiocyanate-labeled antisense *LFY* RNA and red color [P. R. Fobert, E. S. Coen, G. J. P. Murphy, J. H. Doonan, *EMBO J.* **13**, 616 (1994)]. The *TFL1* probe was made with the plasmid pJAM2045. This plasmid contained an internal fragment of ~500 bp of *TFL1*, generated by PCR and subcloned into pGEM-T vector (Promega). The *LFY* probe was made from the plasmid pDW122 as described (20).
  25. Wild-type and *ttf1-1* mutant plants were imbibed at 4°C for 5 days in the dark, before sowing on soil under LD (16 hours light/8 hours dark) or SD (8 hours light/16 hours dark). Plants were transferred at daily intervals from LD to SD and scored when plants had bolted. Assigning leaves to the basal, primary rosette was difficult for plants exhibiting the SD phenotype as secondary shoots developed. This variation was reflected in greater standard errors. SEM analysis confirmed the scoring of plants exhibiting a LD phenotype.
  26. M. H. Williams and P. B. Green, *Protoplasma* **147**, 77 (1988); D. R. Smyth, J. L. Bowman, E. M. Meyerowitz, *Plant Cell* **2**, 755 (1990).
  27. We thank P. Bovill and D. Barker for help in sequencing the *ttf1* alleles; D. Weigel for plasmid pDW122; G. Ingram and R. Simon for advice on manipulation of *Arabidopsis*; R. Schmidt and C. Dean for mapping of the *Arabidopsis* EST; the Arabidopsis Biological Resource Center at Ohio State University (Columbus, OH) and T. Sasaki *et al.* of the Rice Genome Resource Project (Ibaraki, Japan) for clones; E. Schultz for helpful discussions on *TFL1*; and I. Amaya, P. Cubas, and S. Doyle for comments. Supported by grants to E.C. and R.C. from the UK Biotechnology and Biological Sciences Research Council (BBSRC) PMB2 and Stem Cell Programmes, the European Economic Community AMICA program, and Gatsby Foundation. D.B. was also supported by a BBSRC Fellowship and the Sainsbury Laboratory.

15 October 1996; accepted 12 November 1996

## Common Neural Substrates for the Addictive Properties of Nicotine and Cocaine

Emilio Merlo Pich,\* Sonia R. Pagliusi, Michela Tessari, Dominique Talabot-Ayer, Rob Hooft van Huijsduijnen, Christian Chiamulera

Regional brain activation was assessed by mapping of Fos-related protein expression in rats trained to self-administration of intravenous nicotine and cocaine. Both drugs produced specific overlapping patterns of activation in the shell and the core of the nucleus accumbens, medial prefrontal cortex, and medial caudate areas, but not in the amygdala. Thus, the reinforcing properties of cocaine and nicotine map on selected structures of the terminal fields of the mesocorticolimbic dopamine system, supporting the idea that common substrates for these addictive drugs exist.

Nicotine is critical in the maintenance of tobacco smoking (1). Recent observations indicate that nicotine, like cocaine, activates the mesocorticolimbic dopamine (DA) system (2). This suggests similarities between the neuroactive properties of cocaine and nicotine but does not show whether the reinforcing properties of these two drugs involve similar neural substrates.

Experiments with animals that voluntarily press a lever to receive cocaine infusions strongly indicate that the mesocorticolimbic DA system is also a key neuroanatomical substrate for drug-seeking behavior itself (3). Because nicotine is intravenously self-administered in rats (4, 5), a study was designed to investigate whether the same set of neurons, a target

of the mesocorticolimbic DA system, is activated by self-administration of nicotine and of cocaine. Overlaps in brain activation maps between cocaine and nicotine self-administration might identify a common substrate for cocaine and nicotine addiction.

Neuronal activation of the rat brain can be measured by mapping the expression of the immediate-early gene *c-fos* (6). Acute injection of cocaine and nicotine is known to produce transient increases of the expression of *c-fos* protein (Fos) and other Fos-related antigens (FRAs) in the nucleus accumbens and caudate region (7, 8). Newly synthesized Fos and FRAs heterodimerize with members of the Jun family to form the activating protein-1 (AP-1) complexes, which are important transcriptional regulators in neurons (6–9). Some FRAs, such as the 35-kD component, do not behave as immediate-early genes but their products, once induced, may last for several days (9).

Here, a computer-based detailed re-

E. Merlo Pich, S. R. Pagliusi, D. Talabot-Ayer, R. Hooft van Huijsduijnen, Geneva Biomedical Research Institute, Glaxo-Wellcome R&D, CH-1228 Geneva, Switzerland. M. Tessari and C. Chiamulera, Medicines Research Center, Glaxo-Wellcome SpA, 37100 Verona, Italy.

\*To whom correspondence should be addressed.

gional mapping of FRAs-like immunoreactive (FRAs-LI) profiles, as well as measurements of AP-1 binding, were per-

formed in the brain of control rats and in rats killed after the last session of nicotine or cocaine self-administration (10). FRAs-

LI was specifically used because the effects of cocaine on Fos-LI are known to be attenuated by repeated administration (7, 9).

Rats were first trained to press a lever for food, then, after surgical implantation of a catheter in the jugular vein, for intravenous nicotine or cocaine administration (11). The control animals were divided into two main groups: (i) untrained rats, which were exposed to the operant box daily and did not receive any training before or after surgery; and (ii) saline rats, which learned to press the lever for food and then received intravenous saline instead of nicotine or cocaine. An additional group of saline rats, acute nicotine rats, passively received the same amount of intravenous nicotine as rats that were actively self-administering nicotine, but only during the last session. In these animals, nicotine would act on brain structures that produce effects on Fos and FRAs expression that are unlikely to be related to the reinforcing properties of nicotine; indeed, aversive-like effects after

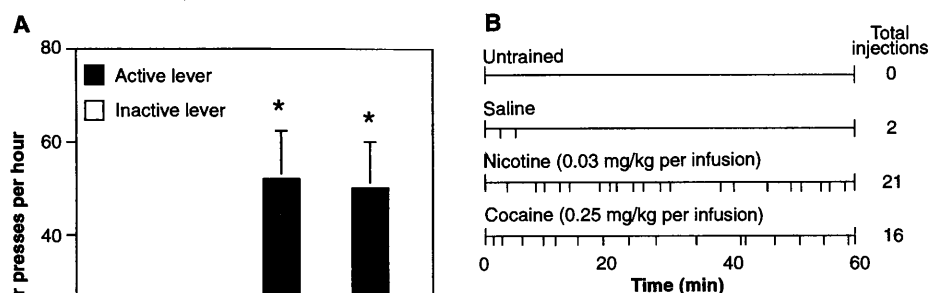


**Fig. 1.** (A) Average responses (active lever presses per hour) for each experimental group ( $n = 4$  to 13 rats) during the last session in operant boxes after a 2-week training period (11). Untr., untrained control rats; Sal., Nic., and Coc. rats trained to lever press for food and then

for intravenous saline, nicotine (0.03 mg/kg per infusion), or cocaine (0.25 mg/kg per infusion), respectively. Asterisk indicates  $P < 0.01$  versus untrained control rats. (B) Self-administration records for one representative animal per group. Each vertical mark indicates the delivery of intravenous infusion after completion of two (cocaine) or three (nicotine and saline) lever responses.

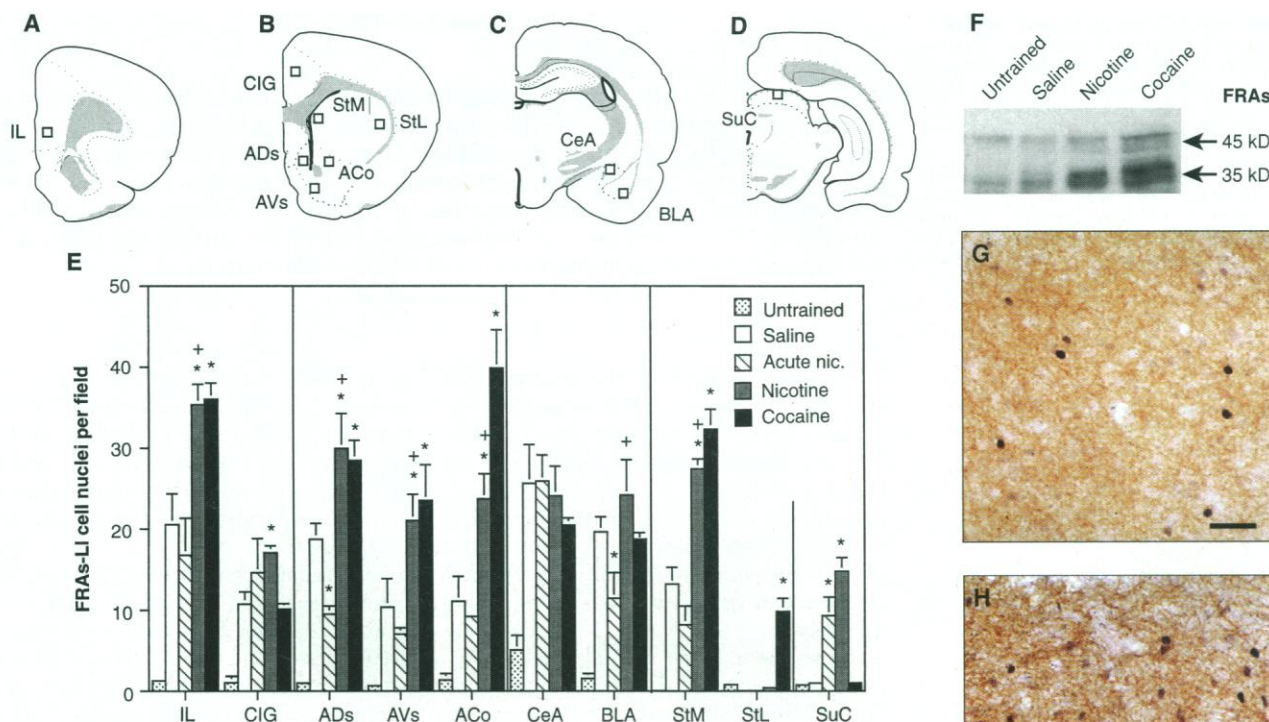


**Fig. 2.** (A through D) Open squares on the brain maps represent the anatomical areas chosen for quantitative image analysis of FRAs-LI profiles. The anteroposterior level of each section is defined as distance from the Bregma in stereotaxic coordinates (79): (A) 2.8 mm; (B) 1.70 mm; (C) -6.00 mm; and (D) -2.45 mm. IL, infralimbic cortex; CIG, anterior cingulate cortex, layers II and III; ADs, nucleus accumbens, dorsal shell; AVs, nucleus accumbens, ventral shell; ACo, nucleus accumbens, core; CeA, central nucleus of amygdala; BLA, basolateral nucleus of amygdala; StM, caudate-putamen, medial part; StL, caudate-putamen, laterodorsal part; and SuC, superficial gray of the superior colliculus. (E) Number of FRAs-LI profiles counted within each anatomical area represented in (A) through (D) of rats killed 90 min after the last self-administration session (10). Analysis of variance (ANOVA) indicated a significant group effect in all the brain regions ( $P < 0.01$ ). Significant differences between groups are indicated as follows: \*,  $P < 0.05$  compared to saline; and +,  $P < 0.05$  compared to acute nicotine. (F) FRA immunoblot of nucleus accumbens microdissected 60 min after the last self-administration session. Experimental groups were as defined as in the legend of Fig. 1. Antibody to FRAs was used at 25  $\mu$ g/ml. (G and H) Representative photomicrographs of FRAs-LI cell nuclei (black-stained dots) in the ventral shell of the nucleus accumbens of one saline rat (G) and one nicotine self-administration rat (H). Scale bar, 20  $\mu$ m.

acute nicotine or cocaine administration are known (12). Lever-press behavior was stably maintained for 2 weeks in rats that received nicotine or cocaine, whereas the performance of saline rats was significantly reduced ( $P < 0.01$ ) and that of untrained rats was almost absent (Fig. 1).

Levels of FRAs-LI in the infralimbic cortex, shell and core of the nucleus accumbens, and medial caudate, but not the amygdala, were significantly increased in rats self-administering nicotine and cocaine when compared with levels in saline rats ( $P < 0.05$ ; Fig. 2E). Nicotine, but not cocaine, strongly activated the superior colliculus and anterior cingulate cortex, whereas cocaine alone was effective in the lateral caudate ( $P < 0.05$ ). Acute nicotine infused to saline rats during the last session produced significant effects in the superior colliculus ( $P < 0.05$ ) and to a lesser extent in the anterior cingulate cortex, reaching the values observed in rats self-administering nicotine (Fig. 2E). Because acute passive administration of nicotine produces the same effects on FRAs-LI as seen here to be produced by self-administration, activation of the superior colliculus may not be related to nicotine-reinforcing properties. Clear-cut differences ( $P < 0.01$ ) between all groups of rats trained to press the lever and those that were untrained were observed in

all structures studied, except for the lateral caudate and superior colliculus. Thus, training for lever pressing produced a certain degree of activation in structures that were strongly activated by drug self-administration. No significant correlation was found between the behavioral performance of each treatment group and the FRAs-LI expression in all the brain structures under study.

Confirmation of these results came from measurements of binding of the AP-1 complex to nuclear DNA in microdissected brain tissue of rats killed 60 min after the last session (13). Both nicotine and cocaine self-administration rats showed significant increases of AP-1 binding in the medial prefrontal cortex and nucleus accumbens when compared with that in saline rats (Fig. 3). These changes were paralleled by increases of the 35-kD FRA bands as detected by immunoblot (Fig. 2F). Differential effects were found in the caudate region, where levels of the AP-1 complex were increased by cocaine but not by nicotine (Fig. 3D) (14).

AP-1 complex binding was also measured in animals killed immediately before the last self-administration session (Fig. 3). These animals were not exposed to the last dose of nicotine or cocaine, and the detection of significant levels of the AP-1 com-

plex indicated the effects of previous repeated exposures to drugs or self-administration procedures. High levels of the AP-1 complex were observed in the nucleus accumbens of cocaine and, to a lesser extent, nicotine self-administration rats ( $P < 0.05$  versus saline rats; Fig. 3C). No difference was measured in the prefrontal cortex region (Fig. 3B). In the caudate region, AP-1 binding was increased in all rats except the untrained ones ( $P < 0.05$ ; Fig. 3D), which indicates a specific long-term effect of lever-press training.

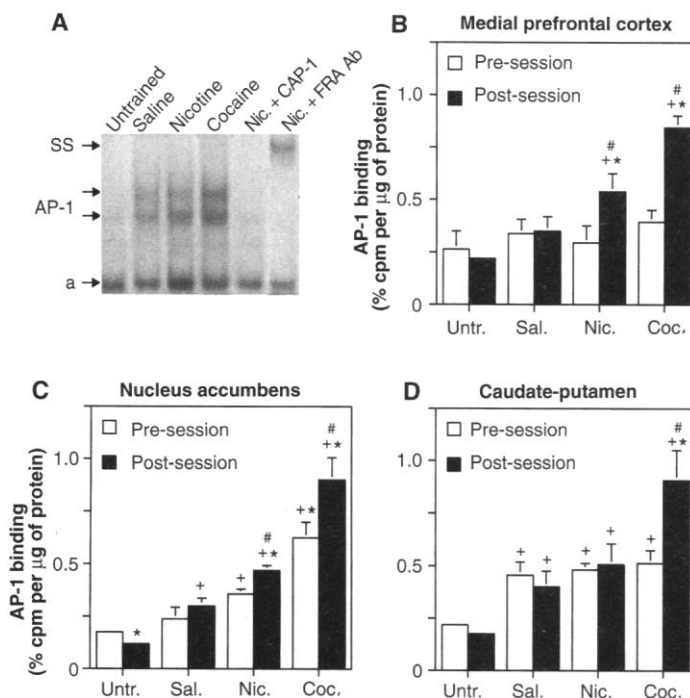
Overall, the data on AP-1 complex binding suggest that each daily session of nicotine or cocaine self-administration produced a fractional increase of FRAs-LI that accumulated particularly in neurons of the nucleus accumbens but not the prefrontal cortex, forming persistent AP-1 complexes. Thus, the transcriptional regulatory effects of persistent AP-1 complexes may be implicated in the long-term adaptive changes associated with the maintenance of nicotine and cocaine self-administration (3, 7, 9).

The pharmacological effects of cocaine on FRAs-LI expression have been described (7, 9); those of nicotine can be related to the increased intracellular calcium levels produced by activation of nicotine receptors located on the glutamate, acetylcholine, or DA terminals projecting to the target areas (2, 15).

In humans, nicotine and cocaine are compulsively self-administered by cigarette smokers and cocaine users (16). In the rat model, compulsive self-administration of nicotine and cocaine was associated with overlapping activation maps in the shell and core of the nucleus accumbens, medial prefrontal cortex, and medial caudate-putamen, but not the amygdala, corroborating the view that there is a common neuronal substrate for addiction to these two drugs.

**Fig. 3. (A)** Representative autoradiogram of a bandshift assay of AP-1 binding in prefrontal cortex extracts of rats killed after the end of the last self-administration session. The lower arrow (a) indicates nonspecific binding; SS indicates the supershifted AP-1 complex band. Specificity experiments were performed in the presence of an excess of AP-1 unlabeled oligonucleotide (0.5 pmol; Nic. + CAP-1) or with the use of a labeled mutant oligonucleotide (19). Supershift experiments were performed by addition of 0.2 ml of antibody to FRAs (Nic. + FRA Ab) (9). Gel bands were directly scanned for radioactivity levels with an Ambis scanner.

**(B through D)** Effects of nicotine and cocaine self-administration on AP-1 levels in various brain regions of rats ( $n = 4$  to 7) killed immediately before (pre-session) or 60 min after (post-session) the last self-administration session. ANOVA indicated a group effect ( $P < 0.05$ ) in the post-session measurements in all three brain structures but indicated a significant pre-session effect only in the nucleus accumbens and caudate-putamen ( $P < 0.05$ ). Significant differences between groups are indicated as follows: \*,  $P < 0.05$  versus saline rats; +,  $P < 0.05$  versus untrained rats; and #,  $P < 0.05$  versus pre-session values.



## REFERENCES AND NOTES

1. J. H. Jaffe and M. Kanzler, *Natl. Inst. Drug Abuse (NIDA) Res. Monogr. Ser. 23* (1979), p. 4; I. P. Stolerman and M. J. Jarvis, *Psychopharmacology* **117**, 2 (1995).
2. P. Calabresi, M. G. Lacey, R. A. North, *Brit. J. Pharmacol.* **98**, 135 (1989); M. Nisell, G. G. Nomikos, T. H. Svensson, *Synapse* **16**, 36 (1994); F. Pontieri et al., *Nature* **382**, 255 (1996).
3. N. E. Goeders and J. E. Smith, *Science* **221**, 773 (1983); G. F. Koob and F. E. Bloom, *ibid.* **242**, 715 (1988); G. Di Chiara, *Drug Alcohol Depend.* **38**, 95 (1995).
4. W. A. Corrigal and K. M. Cohen, *Psychopharmacology* **99**, 473 (1989); W. A. Corrigal, K. B. J. Franklin, K. M. Choen, P. B. S. Clarke, *ibid.* **107**, 285 (1992).
5. M. Tessari, E. Valerio, C. Chiamulera, P. M. Beardsley, *Psychopharmacology* **121**, 282 (1995).
6. S. M. Sagar, F. R. Sharp, T. Curran, *Science* **240**, 1328 (1988); S. M. Morgan and T. Curran, *Annu. Rev. Neurosci.* **14**, 421 (1991).
7. S. T. Young, L. J. Pomino, M. J. Iadarola, *Proc. Natl. Acad. Sci. U.S.A.* **88**, 1291 (1991); B. T. Hope, B. Kosofski, S. H. Hyman, E. J. Nestler, *ibid.* **89**, 5764 (1992).

8. T. Ren and S. M. Sagar, *Brain Res. Bull.* **29**, 589 (1992); Y. Pang, H. Kiba, A. Jayaraman, *Mol. Brain Res.* **20**, 162 (1993).
9. B. T. Hope *et al.*, *Neuron* **13**, 1235 (1994).
10. Rats were anesthetized and transcardially perfused as described (7, 8). Cryosections (35  $\mu\text{m}$ ) were sequentially incubated with antibodies against FRAs (7) (dilution, 1:4000), and tyrosine hydroxylase (TH; dilution 1:500) (Chemicon) was used to stain DA terminals. Detection was performed with avidin-biotin-peroxidase complex (Vector Laboratories), followed by diaminobenzidine for TH and nickel enhancement for FRA signals. The number of positive nuclei was measured within a squared field area of  $270 \times 270 \mu\text{m}$  with the use of the IBAS image analysis system (Zeiss, Germany). Each area was measured in four adjacent coronal sections, and the results were averaged. For details, see M. Zoli *et al.*, *Neurochem. Int.* **16**, 383 (1990).
11. All rats were kept on a restricted diet regime (85% of the normal body weight). Nicotine (0.03 mg per kilogram of body weight) was delivered in a volume of 22  $\mu\text{l}$  per infusion, cocaine (0.25 mg/kg) at 100  $\mu\text{l}$  per infusion, and saline at 22  $\mu\text{l}$  per infusion. These doses were selected among those that can maintain stable self-administration in rats [B. C. Caine and G. F. Koob, *J. Pharmacol. Exp. Ther.* **270**, 209 (1994)] (4, 5). No claim for equipotency of the two drugs was made because direct comparison of the reinforcing effects of cocaine and nicotine requires further studies. Thus, no direct statistical comparison was planned between nicotine and cocaine self-administration groups. Stable baseline performance was defined when the rate of lever pressing between three consecutive sessions did not vary more than 20%.
12. D. D. Flemmer and S. C. Disalver, *Pharmacol. Biochem. Behav.* **34**, 261 (1989); X. M. Yang, A. L. Gorman, A. J. Dunn, N. E. Goeders, *ibid.* **41**, 643 (1992).
13. Brain structures were microdissected from cryostat sections (300  $\mu\text{m}$ ) according to M. Palkowitz and M. J. Brownstein, *IBRO Handb. Ser. Methods Neurosci.* **2**, 1 (1983). Crude nuclear extracts, probe preparation, and bandshift assays were performed as described [M. Becker-André *et al.*, *Eur. J. Biochem.* **206**, 401 (1992)]. The AP-1 probe (GCC GCA AGT GAC TCA GCG CGG G and its complement) was derived from the human metallothionein II A promoter (9).
14. Acute administration of nicotine in saline rats during the last session did not change AP-1 binding in any brain region when compared with that in saline rats (17).
15. D. S. McGehee, M. J. Heath, S. Gelber, P. Devay, L. W. Role, *Science* **269**, 1692 (1995).
16. J. E. Henningfield, K. Miyasato, D. R. Jasinski, *Pharmacol. Biochem. Behav.* **19**, 887 (1983); M. W. Fischman and C. R. Schuster, *Fed. Proc.* **41**, 241 (1982).
17. E. Merlo Pich *et al.*, data not shown.
18. L. W. Swanson, *Brain Maps: Structures of the Rat Brain* (Elsevier, Amsterdam, 1992).
19. When the mutant oligonucleotide (GCC GCA ATG TCA GAC TAG CCG G) was used, no bands were detected (17).
20. We thank M. Iadarola for providing the antibody to FRAs; R. A. North for discussing the manuscript; S. Catsicas, J. Knowles, D. Trist, and E. Ratti for constant support; and S. DeVevey and E. Valerio for excellent technical assistance. All animal procedures conformed to the Guide for the Care and Use of Laboratory Animals (NIH). Part of these data was presented at the Society for Neuroscience meeting [C. Chiamulera *et al.*, *Soc. Neurosci. Abstr.* **21**, 722 (1995)].

2 September 1996; accepted 5 November 1996

## Interaction of the Thiol-Dependent Reductase ERp57 with Nascent Glycoproteins

Jason D. Oliver, Fimme J. van der Wal, Neil J. Bulleid, Stephen High\*

Calnexin and calreticulin interact specifically with newly synthesized glycoproteins in the endoplasmic reticulum (ER) and function as molecular chaperones. The carbohydrate-specific interactions between ER components and glycoproteins synthesized in isolated canine pancreatic microsomes were analyzed using a cross-linking approach. A carbohydrate-dependent interaction between newly synthesized glycoproteins, the thiol-dependent reductase ERp57, and either calnexin or calreticulin was identified. The interaction between ERp57 and the newly synthesized glycoproteins required trimming of the N-linked oligosaccharide side chain. Thus, it is likely that ERp57 functions as part of the glycoprotein-specific quality control machinery operating in the lumen of the ER.

The lumen of the ER contains a number of molecular chaperones that assist in the later stages of protein biosynthesis and folding (1, 2). A number of studies have highlighted specific interactions between newly synthesized glycoproteins and the putative chaperones calnexin and calreticulin (3–6). The binding of calnexin and calreticulin to newly synthesized proteins is normally characterized by a specific requirement for correctly processed, asparagine-linked (N-linked), carbohydrate side chains. In combination with uridine 5'-diphosphate (UDP)-glucose:glycoprotein glucosyltransferase (7), calnexin and calreticulin are thought to mediate a quality control cycle for newly synthesized glycoproteins (2, 8, 9). The function of this cycle is to ensure that only correctly folded and assembled proteins exit the ER and gain access to later compart-

ments of the secretory pathway (2, 10).

Here, we used model substrates derived from the secretory protein preprolactin (PPL) (11) to determine the effect of N-linked glycosylation on the interactions between newly synthesized polypeptides and ER proteins. When the PPL92.CHO transcript was translated *in vitro* in the presence of canine pancreatic microsomes, a glycosylated 62-amino acid prolactin fragment (PL62.CHO) was generated. In contrast, translation of the PPL92.Con transcript generated a nonglycosylated 62-amino acid fragment (PL62.Con). The interactions between both PL62.CHO and PL62.Con and ER components were analyzed with the use of the membrane-permeable cross-linking reagent succinimidyl 4-(N-maleimidomethyl) cyclohexane carboxylate (SMCC), a heterobifunctional reagent that principally cross-links lysines to cysteines. Two groups of cross-linking partners could be identified: (i) ER proteins that interacted with both glycosylated and nonglycosylated polypeptides, exemplified by protein disul-

fide isomerase (PDI) (Fig. 1A); and (ii) ER proteins that interacted only with glycosylated polypeptides. Calnexin and calreticulin, which interact principally with glycoproteins, were observed to cross-link to PL62.CHO (Fig. 1B) but not to PL62.Con (Fig. 1A). A weaker 160-kD product (Fig. 1B) presumably represented a ternary cross-linking adduct of calnexin, PL62.CHO, and a third unidentified component.

In addition to antisera that recognized calnexin, calreticulin, and PDI, a number of antisera to other ER luminal proteins were screened for immunoprecipitation of glycosylation-dependent (that is, PL62.CHO-specific) cross-linking products (12). We were able to identify ERp57 (13), a thiol-dependent reductase (14) and putative cysteine protease (15), as a strong cross-linking partner of PL62.CHO but not of PL62.Con (compare Figs. 1A and 1B). This result suggested that, like calnexin and calreticulin, ERp57 interacts specifically with glycoproteins.

When immunoprecipitation was performed under "native" conditions (6), a 69-kD cross-linking product was coprecipitated with both calnexin and calreticulin (Fig. 1B). This 69-kD product was absent when samples were denatured with SDS before immunoprecipitation (Fig. 1B). The glycosylated PL62.CHO product had an apparent molecular mass of 9 kD (11), which implied that a 60-kD cross-linking partner was coprecipitated with the calnexin and calreticulin cross-linking products. A similar 60-kD calnexin-associated protein, denoted CAP-60, coprecipitates with adducts of the Glut-1 glucose transporter and calnexin (6).

The 69-kD cross-linking product obtained with PL62.CHO had a similar mobility to those obtained with both PDI and ERp57 (Fig. 1B). To establish whether CAP-60 was actually one of these components, we performed sequential immunopre-

School of Biological Sciences, University of Manchester, 2.205 Stopford Building, Oxford Road, Manchester M13 9PT, UK.

\*To whom correspondence should be addressed. E-mail: shigh@fs2.scg.man.ac.uk